Knowledge E
Engaging minds

Conference Paper

Strontium and Iron Substituted Lanthanum Nickelate as Cathode Material in Solid Oxide Fuel Cells

A.R. Gilev, E.A. Kiselev, and V.A. Cherepanov

Institute of Natural Sciences, Ural Federal University, 620000 Ekaterinburg, Russia

Abstract

The MIEC $La_{1.5}Sr_{0.5}Ni_{1-y}Fe_yO_4$ (y=0.1-0.4) oxides have been studied as cathode materials with $La_{0.88}Sr_{0.12}Ga_{0.82}Mg_{0.18}O_{3-\delta}$ (LSGM) electrolyte. Total conductivity, thermal expansion, oxygen nonstoichiometry, and chemical compatibility with LSGM and $Ce_{0.8}Sm_{0.2}O_{1.9}$ (SDC) were determined. The following fuel cells were tested: $La_{1.5}Sr_{0.5}Ni_{1-y}Fe_yO_4$ (y=0.1, 0.2, 0.3, 0.4)/SDC/LSGM/$Sr_2N_{0.75}Mg_{0.25}MoO_6$ (SNMM) and $La_{1.5}Sr_{0.5}Ni_{0.6}Fe_{0.4}O_4$/SDC/LSGM/SDC/NiO-SDC. For the former, the maximum power densities were 218, 274, 222, and 390 mW/cm^2 at 850 °C in case of y equal to 0.1, 0.2, 0.3, and 0.4, respectively. The latter cell showed maximum power density of 341 mW/cm^2 at 850°C.

Keywords: fuel cell, conductivity, thermal expansion, cathodes

🔓 **OPEN ACCESS**

1. Introduction

$La_2NiO_{4+\delta}$ with the K_2NiF_4-type structure is a mixed conductor with large oxygen excess. It is considered as a promising cathode material for solid oxide fuel cells (SOFC) due to a number of advantages such as relatively fast oxygen-ion transport via interstitial oxygen ions, moderate thermal expansion, and high electrocatalytic activity. Nevertheless, it has a few shortcomings such as relatively low total conductivity and chemical incompatibility with various well-known electrolytes [1-3].

The effective way to modify properties in order to improve the cathode characteristics of La_2NiO_4 is chemical doping. An acceptor-type strontium doping of La_2NiO_4 was extensively studied earlier [4-6]. The addition of strontium increases total conductivity of the oxides, although it significantly diminishes oxygen content [5]. The thermal expansion coefficient (TEC) of $La_{2-x}Sr_xNiO_4$ in the 0<x<0.6 range is almost constant and equals to 12-12.5×10^{-6} K^{-1} at 800°C [4]. Donor-type doping of La_2NiO_4 and $La_{2-x}Sr_xNiO_4$ by iron exhibits an opposite effect: gradual decrease of electric conductivity along with the rise of interstitial oxygen concentration [7]. The TEC values slightly increased with addition of iron [8].

Chemical compatibility of La_2NiO_4 with electrolytes such as YSZ, CGO, and LSGM was previously studied [2, 3]. Chemical reactions were observed in case of both YSZ and

How to cite this article: A.R. Gilev, E.A. Kiselev, and V.A. Cherepanov, (2016), "Strontium and Iron Substituted Lanthanum Nickelate as Cathode Material in Solid Oxide Fuel Cells," in *IV Sino-Russian ASRTU Symposium on Advanced Materials and Materials and Processing Technology*, KnE Materials Science, pages 64–70. DOI 10.18502/kms.v1i1.564

Page 64

CGO electrolytes [2]. It was also shown that La_2NiO_4 was not chemically compatible with LSGM electrolyte neither at fabrication conditions nor at operation ones [3].

Thus, the aims of this work are to modify properties of La_2NiO_4 by simultaneous doping with strontium and iron and to estimate the performance of the $La_{1.5}Sr_{0.5}Ni_{1-y}Fe_yO_4$ (y=0.1-0.4) cathodes applied to the LSGM electrolyte-based SOFC.

2. Methods

The series of the $La_{1.5}Sr_{0.5}Ni_{1-y}Fe_yO_{4+\delta}$ complex oxides (y=0.1-0.4) was synthesized via citric-nitric technique as described elsewhere [9]. The phase purity of the samples was confirmed by the XRPD analysis using Equinox 3000 (FWHM $\sim$ 0.05° at 2θ) instrument with Cu-K$_\alpha$ radiation at room temperature (RT). Observed XRPD data were refined by the Le-Bail technique (profile-matching mode) using FullProf software. The absolute values of oxygen non-stoichiometry were obtained in the thermogravimetric analysis (TGA) setup (STA 409PC Netzsch GmbH) by reducing the samples at 1200°C in H_2/N_2 gas mixture with flow rate 100 ml/min. Thermal expansion of $La_{1.5}Sr_{0.5}Ni_{1-y}Fe_yO_{4+\delta}$ was investigated by high-temperature (HT) XRPD in air within 25-1100°C temperature range using HTK 16N (Anton Paar) HT-chamber installed at Equinox 3000 diffractometer. Total conductivity of $La_{1.5}Sr_{0.5}Ni_{1-y}Fe_yO_{4+\delta}$ was measured by the 4-probe DC technique within 25-1100°C temperature range in air. Chemical compatibility of the oxides with electrolyte materials $La_{0.88}Sr_{0.12}Ga_{0.82}Mg_{0.18}O_{3-\delta}$ (LSGM) and $Ce_{0.8}Sm_{0.2}O_{1.9}$(SDC) was studied by mixing the cathode and electrolyte powders in a 1:1 weight ratio, following by calcination at 1250°C for 1 h and XRPD examination.

The powder of $La_{0.88}Sr_{0.12}Ga_{0.82}Mg_{0.18}O_{3-\delta}$ electrolyte was uniaxially pressed into the pellet of 0.7 mm thickness and sintered at 1400°C in air for 20 h. In order to avoid possible chemical interaction between the $La_{1.5}Sr_{0.5}Ni_{1-y}Fe_yO_{4+\delta}$ cathode and the LSGM electrolyte the latter was preliminary coated by a layer of $Ce_{0.8}Sm_{0.2}O_{1.9}$ buffer and sintered at 1300°C in air for 1 h. $Sr_2Ni_{0.75}Mg_{0.25}MoO_{6-\delta}$ (SNMM), as well as NiO-SDC cermet was used as an anode.

The cathode materials were preliminary sonicated in ethanol media for ten minutes to reduce particle size and, thus, intensify a sintering process. The cathode and the anode materials were painted on the opposite sides of the electrolyte pellet and sintered at 1250°C in air for 1 h. In order to separate the anode side, a single fuel cell sandwich with attached Pt-wire current collectors was placed on an YSZ tube and sealed using special high-temperature glass. The fuel H_2 gas was fed inside of the tube with the rate of 250 ml/min. The current-voltage (I–U) characteristics of the cells were measured at 700, 750, 800, and 850°C using a resistance box and the Agilent 34401A multimeter.

Composition	$a=b$, Å	c, Å	V, Å^3	TEC×10^{-6},K^{-} (600-800°C)	δ
y=0	3.81065 [6]	12.7003 [6]	184.422 [6]	12.94 [4]	-0.031 [4]
y=0.1	3.82156(5)	12.72034(21)	185.772(4)	13.72	0.04
y=0.2	3.83244(5)	12.71399(22)	186.738(5)	15.23	0.07
y=0.3	3.83387(10)	12.72142(33)	186.987(8)	14.87	0.09
y=0.4	3.85952(10)	12.69795(36)	189.147(9)	14.59	0.11

TABLE 1: The unit cell parameters, thermal expansion coefficient (TEC) and oxygen non-stoichiometry δ for $La_{1.5}Sr_{0.5}Ni_{1-y}Fe_yO_{4+\delta}$.
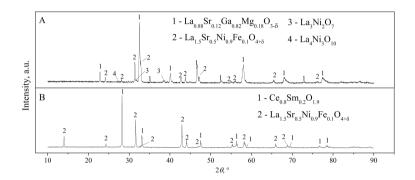

Figure 1: XRPD patterns of $La_{1.5}Sr_{0.5}Ni_{0.9}Fe_{0.1}O_{4+\delta}$-LSGM (A) and $La_{1.5}Sr_{0.5}Ni_{0.9}Fe_{0.1}O_{4+\delta}$-SDC (B) mixtures after calcination at 1250°C for 1 hour.

3. Results

XRPD confirmed that all $La_{1.5}Sr_{0.5}Ni_{1-y}Fe_yO_{4+\delta}$ were single phase (no evidence of impurities or starting materials was detected) possessing tetragonal structure (space group *I4/mmm*). The refined lattice parameters are listed in Table 1.

XRPD pattern of the $La_{1.5}Sr_{0.5}Ni_{0.9}Fe_{0.1}O_{4+\delta}$-SDC mixture after calcination at 1250°C for 1 h exhibits no impurity peaks, indicating that there was no reaction between the cathode and SDC (Fig. 1). On the contrary, XRPD profile of the $La_{1.5}Sr_{0.5}Ni_{0.9}Fe_{0.1}O_{4+\delta}$-LSGM mixture reveals appearance of the lanthanum enriched products related to the $La_3Ni_2O_7$ and $La_4Ni_3O_{10}$ structures (Fig. 1). Because of this interaction, SDC was used as a buffer layer between the cathode and the electrolyte.

Figure 2 illustrates temperature dependencies of total conductivity represented in the form of the $\ln(\sigma T) = f(1/T)$ plots. Total conductivity of the studied oxides shows semiconductor behavior within the whole temperature range studied. The linear $\ln\sigma T = f(1/T)$ dependencies indicate that conductivity in $La_{1.5}Sr_{0.5}Ni_{1-y}Fe_yO_{4+\delta}$ is thermally activated. The activation energy values lay within the 9.7-13 kJ mol^{-1} range, which is characteristic of a small-polaron mechanism [10]. The total conductivity significantly decreases with iron doping, which can be attributed to the hole trapping by iron cations forming stable Fe^{3+} states [10].

The TEC values obtained from the HT XRPD results were calculated in approximation of non-textured polycrystalline materials with randomly oriented crystallites [11] according to the formula presented elsewhere [9]. The intermediate temperature
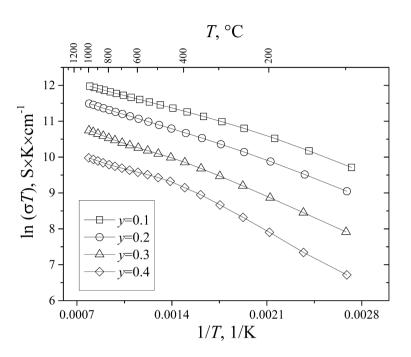
Figure 2: $\ln_\sigma T = f(1/T)$ dependencies of total conductivity for $La_{1.5}Sr_{0.5}Ni_{1-y}Fe_yO_{4+\delta}$ cathodes.

range TEC values calculated from HT XRPD results for $La_{1.5}Sr_{0.5}Ni_{1-y}Fe_yO_{4+\delta}$ are listed in Table 1. One can observe that the TEC values firstly increase with iron doping and then slightly decline at higher iron concentrations. The former phenomenon can be explained by the size factor. Iron substitution leads to an expansion of the unit cell due to larger radius of Fe^{3+} (r=0.645 Å) ions comparing to Ni^{3+} (r=0.56 Å) [12]. As a result, the unit cell volume increases with y, which is followed by a growth of the TEC values. The decrease of the TEC values in case of compositions with y=0.3, 0.4 is due to higher interstitial oxygen concentrations: the release of interstitial oxygen from the structure at elevated temperature suppresses thermal expansion of the material.

The TGA results show that all Fe-substituted $La_{1.5}Sr_{0.5}Ni_{1-y}Fe_yO_{4+\delta}$ accommodate oxygen excess in comparison to $La_{1.5}Sr_{0.5}NiO_{4+\delta}$ [4] (Table 1). The significant increase of oxygen content with *y* can be attributed to the donor-type nature of the dopant: introduction of iron (Fe^{3+}) into the nickel (Ni^{2+}) sublattice increases the trend to incorporate negatively charged interstitial oxygen into the crystal structure in order to preserve electroneutrality.

The electrochemical performances of single fuel cells are shown in Figure 3. The open circuit voltage (OCV) decreases with temperature for all fuel cells. The experimental OCVs were close to the theoretical values for all cells indicating a good densification of the LSGM electrolyte, no gas leakage, and absence of electronic conduction across the electrolyte.

Figure 3 shows typical linear dependencies of the cell voltage vs. current density for the tested cells. One can observe that the output power density for each cell rises with temperature. The maximum values of power density at 850°C in the case of SNMM anode have reached the values: 218, 274, 222, and 390 mW/cm^2 for $La_{1.5}Sr_{0.5}Ni_{0.9}Fe_{0.1}O_{4+\delta}$ (LSFN1), $La_{1.5}Sr_{0.5}Ni_{0.8}Fe_{0.2}O_{4+\delta}$ (LSFN2), $La_{1.5}Sr_{0.5}Ni_{0.7}Fe_{0.3}O_{4+\delta}$
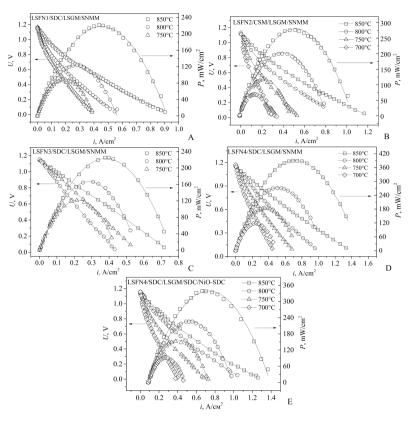
Figure 3: Voltage and power density versus current density for the fabricated fuel cells in H_2 and static air at different temperatures.

(LSFN3), and $La_{1.5}Sr_{0.5}Ni_{0.6}Fe_{0.4}O_{4+\delta}$ (LSFN4) cathodes, respectively. The maximum power density at 850°C in the case of NiO-SDC anode was equal to 341 mW/cm^2 for the $La_{1.5}Sr_{0.5}Ni_{0.6}Fe_{0.4}O_{4+\delta}$ (LSFN4) cathode.

It can be concluded that despite the significant decrease of total conductivity, the performance of the $La_{1.5}Sr_{0.5}Ni_{1-y}Fe_yO_{4+\delta}$ cathodes has been improved with the iron doping. This could be attributed to an increase of interstitial oxygen concentration with y, which, in its turn, benefits the oxygen-ion transport in the oxides [13].

The performance of the $La_{1.5}Sr_{0.5}Ni_{0.6}Fe_{0.4}O_{4+\delta}$/SDC/LSGM/SDC/NiO-SDC cell is slightly improved in comparison with reported earlier results on the La_2NiO_4/LSGM/SDC /Ni-SDC system (319 mW/cm^2 at 850°C) [14]. However, it is important to notice that thickness of the electrolyte in Ref. [14] was 0.4 mm, which is almost twice thinner than that used in our study (0.7 mm). The reducing of the electrolyte thickness could significantly increase the power densities of SOFC with the $La_{1.5}Sr_{0.5}Ni_{0.6}Fe_{0.4}O_{4+\delta}$ cathode.

4. Conclusion

The $La_{1.5}Sr_{0.5}Ni_{1-y}Fe_yO_{4+\delta}$ complex oxides (y=0.1-0.4) have been investigated as cathode materials for potential application in SOFC with the LSGM electrolyte. The XRPD results showed chemical incompatibility of the oxides with LSGM. In order to avoid chemical reaction between the cathode and the electrolyte material, using of the

$Ce_{0.8}Sm_{0.2}O_{1.9}$ buffer layer was necessary. Total conductivity of $La_{1.5}Sr_{0.5}Ni_{1-y}Fe_yO_{4+\delta}$ decreases with iron doping, but the obtained values are still adequate for that required for cathode materials at SOFC [15]. The highest conductivity equal to 130 S/cm at 800°C was achieved for $La_{1.5}Sr_{0.5}Ni_{0.9}Fe_{0.1}O_{4+\delta}$. The thermal expansion coefficients are close to that for LSGM electrolyte (12×10^{-6} K^{-1}). Although the TEC values increase with iron content, high thermal stability is still retained. The oxygen content was shown to increase with y.

The LSGM electrolyte-based fuel cells with the $La_{1.5}Sr_{0.5}Ni_{1-y}Fe_yO_{4+\delta}$ (y=0.1-0.4) cathodes have been assembled. The best performances of 390 mW/cm^2 and 341 mW/cm^2 at 850°C were achieved for the $La_{1.5}Sr_{0.5}Ni_{0.6}Fe_{0.4}O_{4+\delta}$ cathode in pair with $Sr_2Ni_{0.75}Mg_{0.25}MoO_6$ and NiO-SDC cermet anodes, respectively.

Finally, it can be concluded that simultaneous strontium and iron doping can improve the performance of the La_2NiO_4-based cathode material. One would expect a significant increase of power densities in comparison with the prototype while using a thin-film electrolyte.

Acknowledgement

References

[1] S. Yoo, S. Choi, J. Shin, M. Liu, and G. Kim, Electrical properties, thermodynamic behavior, and defect analysis of La n+1Ni nO 3n+1+δ infiltrated into YSZ scaffolds as cathodes for intermediate-temperature SOFCs, *RSC Advances*, **2**, no. 11, 4648–4655, (2012).

[2] A. Montenegro-Hernández, J. Vega-Castillo, L. Mogni, and A. Caneiro, Thermal stability of Ln2NiO4+δ (Ln: La, Pr, Nd) and their chemical compatibility with YSZ and CGO solid electrolytes, *International Journal of Hydrogen Energy*, **36**, no. 24, 15704–15714, (2011).

[3] N. Solak, M. Zinkevich, and F. Aldinger, Compatibility of La2NiO4 cathodes with LaGaO3 electrolytes: A computational approach, *Solid State Ionics*, **177**, no. 19-25, 2139–2142, (2006).

[4] A. Aguadero, M. J. Escudero, M. Pérez, J. A. Alonso, V. Pomjakushin, and L. Daza, Effect of Sr content on the crystal structure and electrical properties of the system La2-xSrxNiO4+δ (0 ≤ x ≤ 1), *Dalton Transactions*, no. 36, 4377–4383, (2006).

[5] L. V. Makhnach, V. V. Pankov, and P. Strobel, High-temperature oxygen non-stoichiometry, conductivity and structure in strontium-rich nickelates La2-xSrxNiO4-δ (x = 1 and 1.4), *Materials Chemistry and Physics*, **111**, no. 1, 125–130, (2008).

[6] Y. Takeda, R. Kanno, M. Sakano, O. Yamamoto, M. Takano, Y. Bando, H. Akinaga, K. Takita, and J. B. Goodenough, Crystal chemistry and physical properties of La2-xSrxNiO4 (0 ≤ x ≤ 1.6), *Materials Research Bulletin*, **25**, no. 3, 293–306, (1990).

[7] R. Benloucif, N. Nguyen, J. M. Greneche, and B. Raveau, La2-xSrxNi1-yFeyO4-[(x-y) 2]+δ: Relationships between oxygen non-stoichiometry and magnetic and electron transport properties, *Journal of Physics and Chemistry of Solids*, **52**, no. 2, 381–387, (1991).

[8] V. V. Kharton, A. V. Kovalevsky, M. Avdeev, E. V. Tsipis, M. V. Patrakeev, A. A. Yaremchenko, E. N. Naumovich, and J. R. Frade, Chemically induced expansion of La2NiO4+δ-based materials, *Chemistry of Materials*, **19**, no. 8, 2027–2033, (2007).

[9] A. R. Gilev, E. A. Kiselev, and V. A. Cherepanov, Synthesis, oxygen nonstoichiometry and total conductivity of (La,Sr)$_2$ (Mn,Ni)O$_{4\pm\delta}$, *Solid State Ionics*, **279**, 53–59, (2015).

[10] V. V. Kharton, E. V. Tsipis, E. N. Naumovich, A. Thursfield, M. V. Patrakeev, V. A. Kolotygin, J. C. Waerenborgh, and I. S. Metcalfe, Mixed conductivity, oxygen permeability and redox behavior of K2NiF4-type La2Ni0.9Fe0.1O4+δ, *Journal of Solid State Chemistry*, **181**, no. 6, 1425–1433, (2008).

[11] C. N. Munnings, S. J. Skinner, G. Amow, P. S. Whitfield, and I. J. Davidson, Structure, stability and electrical properties of the La(2-x)SrxMnO4±δ solid solution series, *Solid State Ionics*, **177**, no. 19-25, 1849–1853, (2006).

[12] RT. Shannon and Prewitt. , CT: Revised effective ionic radii and systematic studies of interatomic distances in halides and chaleogenides. Acta Crystallogr Sect, in *Prewitt CT: Revised effective ionic radii and systematic studies of interatomic distances in halides and chaleogenides. Acta Crystallogr Sect*, **32**, 751–767, 751–767, 32, 1976.

[13] M. V. Patrakeev, E. N. Naumovich, V. V. Kharton, A. A. Yaremchenko, E. V. Tsipis, P. Núñez, and J. R. Frade, Oxygen nonstoichiometry and electron-hole transport in La 2Ni0.9Co0.1O4+δ, *Solid State Ionics*, **176**, no. 1-2, 179–188, (2005).

[14] M. J. Escudero, A. Fuerte, and L. Daza, La2NiO4+δ potential cathode material on La 0.9Sr0.1Ga0.8Mg0.2O2.85 electrolyte for intermediate temperature solid oxide fuel cell, *Journal of Power Sources*, **196**, no. 17, 7245–7250, (2011).

[15] C. Sun, R. Hui, and J. Roller, Cathode materials for solid oxide fuel cells: A review, *Journal of Solid State Electrochemistry*, **14**, no. 7, 1125–1144, (2010).